# Constraining Geometric JunoCam Parameters by Locally Accurate RGB Alignment of Single Marble Movie Images

Gerald Eichstädt

October 27, 2017

**Abstract**

Aligning the centroids of a single RGB "marble movie" JunoCam image for each of the three filters reduces the degrees of freedom of a given camera model by four. Approximate values for the other degrees of freedom of the camera model result in a locally accurate RGB alignment. [1]


[1]This document was typeset with LaTeX.

# Contents

# 1 Introduction

Juno's Education and Outreach camera JunoCam [3] has taken more than ten thousand images of Jupiter in 2016 and 2017, where Jupiter is seen from a distance. The subset of RGB images provides several related approaches for camera calibration. One basic approach reduces the degrees of freedom of a given camera model by four: On the basis of an assumed camera model, for each of the three color channels, the respective x- and y-coordinates of the centroids of a Jupiter "marble" are determined. By a pseudo-Newton method, four chosen camera model parameters are optimised in a way, that deltas for x- any y-coordinates of the centroids are reduced to small subpixel values. This approach is remotely related to the far more advanced calibration methods applied in the Gaia [4] project.

The raw images have been made available periodically on the missionjuno website [5] for processing by the public. Calibration examples in this article are based on Perijove-08 approach images.

JunoCam was built and is operated by Malin Space Science Systems (MSSS) in San Diego/California.

# 2 Considered Camera Parameters

The calibration method described in this article is independent of the specific camera model. Nevertheless, this section sketches a camera model, since actual calibration runs have been performed on the basis of a specifc family of camera models.

Pixels are assumed to be rectangular tiles of equal size forming a periodic grid. Lengths are expressed in terms of the with of a pixel, since absolute lengths cannot be determined with the means of the described calibration method.

The calibration method assumes Jupiter's distance to be infinite. With this assumption, no navigation data are required, except the spacecraft's rotation. As unit of time, the camera's interframe delay is used. Absolute time isn't required nor assumed to be known.

The considered camera model assumes a spacecraft rotation around one fixed axis, and with a constant angular velocity in terms of interframe delay time units.

The considered family of camera models is assumed to be parameterized by

**FramesPerRot** defines the number of interframe delay time in units per spacecraft revolution,

**ScaleFactor** for the green image, it defines the z-distance of the pinhole from the detector plane in units of pixel widths,

**CenterX** defines the x-position of the optical axis in units of pixel widths relative to the left-most pixel row,

**CenterY** defines the y-position of the optical axis in units of pixel widths relative to the bottom-most pixel row,

**K1** defines the first Brownian [2], [1] radial distortion coefficient,

**K2** defines the second Brownian radial distortion coefficient,

**RotOffsetZ** defines the rotation of the pixel grid around the z-axis in radians relative to the coordinate system induced by the assumed spacecraft rotation axis,

**ScaleErrorRed** defines the relative error of the red ScaleFactor with respect to the green ScaleFactor,

**ScaleErrorBlue** defines the relative error of the blue ScaleFactor with respect to the green ScaleFactor,

**ScaleErrorY** defines the relative error of the pixel hight with respect to the pixel width.

The pinhole camera model is applied first, then ScaleErrors, where $1 + \text{ScaleErrorY}$ is multiplied with $1 + \text{ScaleError}$ for red and blue. Browinan radial distortion is applied to the resulting modified pinhole model.

The layout of the readout regions is derived from information as provided in JunoCam's instrument kernel within the collection of Juno SPICE [6] kernels [7].

The following assumptions about the camera model are implicit, but may deviate from physical reality:

1. The optical axis of the camera is assumed to be perpendicular to the rotation axis of the spacecraft.
2. Higher Brwonian radial distortion coefficients are assumed to be zero.
3. The Brownian distortion is assumed to be the same for all wavelengths.
4. The optical axis of the camera is assumed to be perpendicular to the detector plane.
5. The spacecraft is assumed to perform no (torque-free) precession, nor oscillations.

Since the calibration method is underdetermined, unconsidered parameters show up as modeled parameters deviating from physical values.

# 3 Calibration Method

## 3.1 Jupiter Centroids

Immediately from the respective raw JunoCam ”marble movie” RGB image, an RGB image is rendered with double precision floating point arithmetics. For all renditions within a calibration run, the same rendering conventions are applied.

The actual rendering method isn’t assumed to be essential in detail. But some properties of the rendering method applied to raws this article is based on are mentioned for completeness:

- Raw data are decompanded according to fixed decompanding map as supplied by MSSS and published in SPICE.
- Camera artifacts are neither corrected, nor invalidatedn nor patched.
- Images are rendered in spherical coordinates, with spacecraft rotation axis as the symmetry axis of the spherical coordinate system. Longitude/latitudes squares are squares in the rendered image.
- Images used for centroid calculations are rendered with 120 pixels per longitude and latitude degree of the spherical output coordinate system.
- The value of a raw pixel is weighted linearly according to its vertical pixel distance from the according framelet boundary.
- Linear radiometric weights applied to decompanded raw data are 0.82 for red, 1.0 for green, and 2.17 for blue. This may induce a slightly greenish cast.
- Pixels are interpolated in a bilinear way, where only the four nearest-most pixels of the theoretical raw pixel position are used to calculate the weighted mean decompanded value.
- Color channels are not mixed, but each channel is handled separately.
- Calculations are based on decompanded, radiometrically adjusted, and square-root encoded data.

For each of the three color channels the centroid is calculated within a square. The edge length of the square is six times the standard deviation of the distance of the pixel positions to the centroid weighted by reduced pixel brightness. The first draft centroid position is determined within a crop of 12x12 degrees around the largest bright object in a low-resolution (6 pixels per degree) draft rendition of the whole raw image.

The reduced pixel brightness is defined by the input pixel brightness minus a background level, somewhat arbitrarily set to 20.0 in the considered calibration runs. For the final calculation of the centroid positions, the same background level is subtracted, in order to reduce effects by image noise.

The centroid position of each color channel, as well as the standard deviation are calculated with decompanded, radiometrically adjusted, and square-root encoded double-precision floating point data.

Figure 1 shows a raw input image #07C00543, the first RGB image of the perijove-08 approach sequence. Figure 2 shows the low-resolution rendered draft of image #07C00543. Figure 3 shows the copped draft of image #07C00543, which the first accurate centroid calculations can be based on.

Figure 1: Raw perijove-08 approach image JNCE_2017238_07C00543_V01-raw. Credit: NASA / JPL-Caltech / SwRI / MSSS.

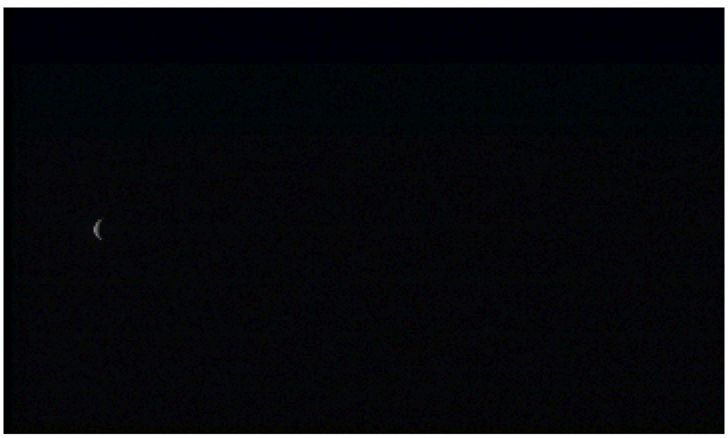

Figure 2: Low-resolution draft rendition of perijove-08 approach image JNCE_2017238_07C00543_V01-raw. Credit: NASA / JPL-Caltech / SwRI / MSSS / Gerald Eichstädt.

Figure 3: Cropped rendition of perijove-08 approach image JNCE_2017238_07C00543_V01-raw. This is a copy of the image for centroid calculation. Actual calculations are performed on a double-precision floating point in-memory version. Credit: NASA / JPL-Caltech / SwRI / MSSS / Gerald Eichstädt.

## 3.2 Applying a Pseudo-Newton Method

For $k \in \mathbf{N}$, and a function

$$F : \mathbf{R}^k \to \mathbf{R}^k,$$

a Newton method iterates the formula

$$x_{n+1} := x_n - (\mathbf{J}F(x_n))^{-1} \cdot F(x_n). \tag{1}$$

In sufficiently linear cases, with the Jacobi matrix $\mathbf{J}F(x_n)$ sufficiently distinctly regular, and with a good choice of the start value $x_0$, this method approximates a zero of $F$.

Call the pixel positions of the centroids of the red, green, and blue channel of a rendered Jupiter marble movie image $(r_x, r_y)$, $(g_x, g_y)$, and $(b_x, b_y)$. Then the constraint, that the centroids of Jupiter in the three color channels should be at the same pixel position, can be stated as

$$\begin{pmatrix} r_x - g_x \\ r_y - g_y \end{pmatrix} = \begin{pmatrix} 0 \\ 0 \end{pmatrix} \text{ and } \begin{pmatrix} b_x - g_x \\ b_y - g_y \end{pmatrix} = \begin{pmatrix} 0 \\ 0 \end{pmatrix}. \tag{2}$$

Choose four parameters of the chosen paramerized family of camera models, and define $F$ as the function that maps these four parameters to the four alignment errors

$$\begin{pmatrix} r_x - g_x \\ r_y - g_y \\ b_x - g_x \\ b_y - g_y \end{pmatrix} \tag{3}$$

of the resulting Jupiter centroids.

Then, with $k = 4$,

$$F : \mathbf{R}^4 \to \mathbf{R}^4$$

is formally valid for an application of the Newton method. The Jacobi matrix $\mathbf{J}F(x_n)$ remains to be determined. Instead of an analytical approach, $\mathbf{J}F(x_n)$ is approximated numerically, which makes the method a pseudo-Newton method.

For parameters $p_1, p_2, p_3, p_4 \in \mathbf{R}$, and small $\delta_1, \delta_2, \delta_3, \delta_4 \in \mathbf{R}$, the four difference quotients

$$\frac{F(p_1 + \delta_1, p_2, p_3, p_4) - F(p_1 - \delta_1, p_2, p_3, p_4)}{2 \cdot \delta_1},$$

$$\frac{F(p_1, p_2 + \delta_2, p_3, p_4) - F(p_1, p_2 - \delta_2, p_3, p_4)}{2 \cdot \delta_2},$$

$$\frac{F(p_1, p_2, p_3 + \delta_3, p_4) - F(p_1, p_2, p_3 - \delta_3, p_4)}{2 \cdot \delta_3},$$

and

$$\frac{F(p_1, p_2, p_3, p_4 + \delta_4) - F(p_1, p_2, p_3, p_4 - \delta_4)}{2 \cdot \delta_4}$$

are vectors with four entries, each. Together, the resulting $4 \times 4$-Matrix is used as an approximation of the Jacobi-Matrix. This requires the rendition of eight versions of the considered marble movie image, for each iteration of the pseudo-Newton method.

The following table is split due to its width. It shows centroid positions determined for an initial set of parameters in row 0. Then from row 1 to row 20, pairs consisting of one parameter varied, and according centroid positions. Row 21 shows the resulting parameters and centroid positions after applying one pseudo-Newton iteration step, based on the difference quotients obtained from the variation of four paramters FramesPerRot, CenterX, CenterY, and RotOffsetZ.

| row | FramesPerRot | ScaleFactor | CenterX | CenterY |
|---|---|---|---|---|
| 0 | 80.870000 | 1478.000000 | 814.000000 | 600.000000 |
| 1 | 80.868000 | 1478.000000 | 814.000000 | 600.000000 |
| 2 | 80.872000 | 1478.000000 | 814.000000 | 600.000000 |
| 3 | 80.870000 | 1477.800000 | 814.000000 | 600.000000 |
| 4 | 80.870000 | 1478.200000 | 814.000000 | 600.000000 |
| 5 | 80.870000 | 1478.000000 | 812.000000 | 600.000000 |
| 6 | 80.870000 | 1478.000000 | 816.000000 | 600.000000 |
| 7 | 80.870000 | 1478.000000 | 814.000000 | 598.000000 |
| 8 | 80.870000 | 1478.000000 | 814.000000 | 602.000000 |
| 9 | 80.870000 | 1478.000000 | 814.000000 | 600.000000 |
| 10 | 80.870000 | 1478.000000 | 814.000000 | 600.000000 |
| 11 | 80.870000 | 1478.000000 | 814.000000 | 600.000000 |
| 12 | 80.870000 | 1478.000000 | 814.000000 | 600.000000 |
| 13 | 80.870000 | 1478.000000 | 814.000000 | 600.000000 |
| 14 | 80.870000 | 1478.000000 | 814.000000 | 600.000000 |
| 15 | 80.870000 | 1478.000000 | 814.000000 | 600.000000 |
| 16 | 80.870000 | 1478.000000 | 814.000000 | 600.000000 |
| 17 | 80.870000 | 1478.000000 | 814.000000 | 600.000000 |
| 18 | 80.870000 | 1478.000000 | 814.000000 | 600.000000 |
| 19 | 80.870000 | 1478.000000 | 814.000000 | 600.000000 |
| 20 | 80.870000 | 1478.000000 | 814.000000 | 600.000000 |
| 21 | 80.896880 | 1478.000000 | 833.254788 | 611.600585 |

| row | K1 | K2 | RotOffsetZ |
|---|---|---|---|
| 0 | -0.000000038000000 | 0.0000000000000002600000000 | 0.000000 |
| 1 | -0.000000038000000 | 0.0000000000000002600000000 | 0.000000 |
| 2 | -0.000000038000000 | 0.0000000000000002600000000 | 0.000000 |
| 3 | -0.000000038000000 | 0.0000000000000002600000000 | 0.000000 |
| 4 | -0.000000038000000 | 0.0000000000000002600000000 | 0.000000 |
| 5 | -0.000000038000000 | 0.0000000000000002600000000 | 0.000000 |
| 6 | -0.000000038000000 | 0.0000000000000002600000000 | 0.000000 |
| 7 | -0.000000038000000 | 0.0000000000000002600000000 | 0.000000 |
| 8 | -0.000000038000000 | 0.0000000000000002600000000 | 0.000000 |
| 9 | -0.000000039000000 | 0.0000000000000002600000000 | 0.000000 |
| 10 | -0.000000037000000 | 0.0000000000000002600000000 | 0.000000 |
| 11 | -0.000000038000000 | 0.0000000000000002200000000 | 0.000000 |
| 12 | -0.000000038000000 | 0.0000000000000003000000000 | 0.000000 |
| 13 | -0.000000038000000 | 0.0000000000000002600000000 | -0.000500 |
| 14 | -0.000000038000000 | 0.0000000000000002600000000 | 0.000500 |
| 15 | -0.000000038000000 | 0.0000000000000002600000000 | 0.000000 |
| 16 | -0.000000038000000 | 0.0000000000000002600000000 | 0.000000 |
| 17 | -0.000000038000000 | 0.0000000000000002600000000 | 0.000000 |
| 18 | -0.000000038000000 | 0.0000000000000002600000000 | 0.000000 |
| 19 | -0.000000038000000 | 0.0000000000000002600000000 | 0.000000 |
| 20 | -0.000000038000000 | 0.0000000000000002600000000 | 0.000000 |
| 21 | -0.000000038000000 | 0.0000000000000002600000000 | 0.002045 |

| row | ScaleErrorRed | ScaleErrorBlue | ScaleErrorY |
|---|---|---|---|
| 0 | 0.000000000000 | 0.000000000000 | 0.000000000000 |
| 1 | 0.000000000000 | 0.000000000000 | 0.000000000000 |
| 2 | 0.000000000000 | 0.000000000000 | 0.000000000000 |
| 3 | 0.000000000000 | 0.000000000000 | 0.000000000000 |
| 4 | 0.000000000000 | 0.000000000000 | 0.000000000000 |
| 5 | 0.000000000000 | 0.000000000000 | 0.000000000000 |
| 6 | 0.000000000000 | 0.000000000000 | 0.000000000000 |
| 7 | 0.000000000000 | 0.000000000000 | 0.000000000000 |
| 8 | 0.000000000000 | 0.000000000000 | 0.000000000000 |
| 9 | 0.000000000000 | 0.000000000000 | 0.000000000000 |
| 10 | 0.000000000000 | 0.000000000000 | 0.000000000000 |
| 11 | 0.000000000000 | 0.000000000000 | 0.000000000000 |
| 12 | 0.000000000000 | 0.000000000000 | 0.000000000000 |
| 13 | 0.000000000000 | 0.000000000000 | 0.000000000000 |
| 14 | 0.000000000000 | 0.000000000000 | 0.000000000000 |
| 15 | 0.000010000000 | 0.000000000000 | 0.000000000000 |
| 16 | 0.000010000000 | 0.000000000000 | 0.000000000000 |
| 17 | 0.000000000000 | -0.000010000000 | 0.000000000000 |
| 18 | 0.000000000000 | 0.000010000000 | 0.000000000000 |
| 19 | 0.000000000000 | 0.000000000000 | -0.000010000000 |
| 20 | 0.000000000000 | 0.000000000000 | 0.000010000000 |
| 21 | 0.000000000000 | 0.000000000000 | 0.000000000000 |

| row | x_red | y_red | x_green | y_green | x_blue | y_blue |
|---|---|---|---|---|---|---|
| 0 | 746.259595 | 708.511135 | 747.314548 | 708.488914 | 747.516670 | 707.485232 |
| 1 | 746.259325 | 708.590907 | 747.313809 | 708.549130 | 747.516631 | 707.525139 |
| 2 | 746.259481 | 708.431491 | 747.315616 | 708.428833 | 747.516831 | 707.445477 |
| 3 | 745.941187 | 708.353591 | 746.992237 | 708.440049 | 747.189823 | 707.537591 |
| 4 | 746.575580 | 708.667947 | 747.635439 | 708.541387 | 747.840336 | 707.424412 |
| 5 | 754.460631 | 708.620628 | 755.601796 | 708.524804 | 755.802841 | 707.443282 |
| 6 | 738.062870 | 708.401490 | 739.032349 | 708.454679 | 739.233553 | 707.519835 |
| 7 | 745.795636 | 717.739852 | 747.195121 | 717.898504 | 747.690611 | 716.886621 |
| 8 | 746.723553 | 699.282188 | 747.440879 | 699.084567 | 747.344995 | 698.080091 |
| 9 | 745.166940 | 707.971002 | 746.386322 | 708.343029 | 746.570154 | 707.656500 |
| 10 | 747.348072 | 709.045148 | 748.241624 | 708.634338 | 748.461653 | 707.315677 |
| 11 | 746.065455 | 708.414307 | 747.174471 | 708.465178 | 747.372986 | 707.508557 |
| 12 | 746.452201 | 708.608542 | 747.454424 | 708.511732 | 747.658732 | 707.458449 |
| 13 | 746.840574 | 707.120104 | 747.473427 | 707.086154 | 747.301066 | 706.076401 |
| 14 | 745.675967 | 709.895522 | 747.158883 | 709.898377 | 747.731092 | 708.890124 |
| 15 | 746.236174 | 708.499519 | 747.314548 | 708.488914 | 747.516670 | 707.485232 |
| 16 | 746.282997 | 708.522752 | 747.314548 | 708.488914 | 747.516670 | 707.485232 |
| 17 | 746.259595 | 708.511135 | 747.314548 | 708.488914 | 747.492608 | 707.489377 |
| 18 | 746.259595 | 708.511135 | 747.314548 | 708.488914 | 747.540674 | 707.480980 |
| 19 | 746.260310 | 708.499620 | 747.314925 | 708.485182 | 747.516763 | 707.489548 |
| 20 | 746.258869 | 708.522664 | 747.314171 | 708.492646 | 747.516578 | 707.480918 |
| 21 | 667.924154 | 658.722915 | 667.887495 | 658.698651 | 667.844346 | 658.675866 |

While the initial alignment errors in row 0 have been

$$\begin{pmatrix} 746.259595 - 747.314548 \\ 708.511135 - 708.488914 \\ 747.516670 - 747.314548 \\ 707.485232 - 708.488914 \end{pmatrix} = \begin{pmatrix} -1.054953 \\ 0.022221 \\ 0,202122 \\ -1,003682 \end{pmatrix}, \tag{4}$$

in row 21, after the first iteration, these errors are

$$\begin{pmatrix} 667.924154 - 667.887495 \\ 658.722915 - 658.698651 \\ 667.844346 - 667.887495 \\ 658.675866 - 658.698651 \end{pmatrix} = \begin{pmatrix} 0.036659 \\ 0.024264 \\ -0.043149 \\ -0.022785 \end{pmatrix}. \tag{5}$$

The maximum norm, defined by $\left\| \begin{pmatrix} x_1 \\ \vdots \\ x_k \end{pmatrix} \right\|_\infty := \max\{|x_1|, \dots, |x_k|\}$, improved from 1.054953 to 0.043149, which means an improvement of alignment accuracy in terms of the maximum norm of a factor of about 24.

The next two iteration steps result in

- FramesPerRot=80.897941,

- ScaleFactor=1478.000000,
- CenterX= 833.582258,
- CenterY= 611.609518,
- K1=-0.000000038000000,
- K2= 0.000000000000002600000000,
- RotOffsetZ= 0.002107,
- ScaleErrorRed= 0.000000000000,
- ScaleErrorBlue= 0.000000000000,
- ScaleErrorY= 0.000000000000,
- x0= 746.518708,
- y0= 719.796932,
- x1= 746.520894,
- y1= 719.804896,
- x2= 746.519305,
- y2= 719.802380,

and

- FramesPerRot=80.897883,
- ScaleFactor=1478.000000,
- CenterX= 833.673575,
- CenterY= 611.734550,
- K1=-0.000000038000000,
- K2= 0.000000000000002600000000,
- RotOffsetZ= 0.002134,
- ScaleErrorRed= 0.000000000000,
- ScaleErrorBlue= 0.000000000000,
- ScaleErrorY= 0.000000000000,

- x0= 746.142551,
- y0= 719.297888,
- x1= 746.144814,
- y1= 719.295555,
- x2= 746.143252,
- y2= 719.296657.

The misalignment after the third pseudo-Newton iteration is

$$\begin{pmatrix} 746.142551 - 746.144814 \\ 719.297888 - 719.295555 \\ 746.143252 - 746.144814 \\ 719.296657 - 719.295555 \end{pmatrix} = \begin{pmatrix} -0.002263 \\ 0.002333 \\ -0.001562 \\ 0.001102 \end{pmatrix}, \tag{6}$$

hence a maximum norm of 0.002333. Since these alignment errors have been determined in renditions with 120 pixels per degree rather than about the 30 pixels per degree of the raw images, this maximum norm corresponds to a misalignment maximum norm of the considered example centroid of about 0.0005 raw pixels.

This highly accurate result is of course specific to the rendition method, the way to define centroids, and it needs to be determined anew for each marble movie image. Even then, the calibration is only valid for the particular centroid position. However, with the other parameters chosen reasonably, the local area of good alignment can be extended sufficiently far to obtain acceptable global RGB alignment.

Figure 4 compares the rendition of image #07C00543 before, and after calibration. The lower row is about 8-fold saturation enhanced. Comparing the limbs reveals a considerable improvement.

Figure 4: Comparison of pre- and post-calibration rendition of perijove-08 approach image JNCE_2017238_07C00543_V01-raw. The lower row is 8-fold saturation enhanced, in order to reveal RGB alignment inaccuracies. Credit: NASA / JPL-Caltech / SwRI / MSSS / Gerald Eichstädt.

# 4 Limitations and Future Work

## 4.1 Systematic Errors by Jupiter's Non-Uniform Color

A closer inspection of figure 4 reveals, that the calibrated image still isn't aligned perfectly in terms of the overall shape of Jupiter. The residual discrepancy with the centroid alignment appears to be an effect of the non-uniform colorization of Jupiter. In the example, the lower part of Jupiter appears cast to yellowish, while the upper part appears to be cast to bluish. Alignment of the centroids results in a small displacement of the blue centroid towards the bottom, resulting in a yellowish upper limb, and a bluish lower limb. Modeling Jupiter's colors on the basis of closer-up images bears the potential to adjust centroid alignment by systematic errors induced by Jupiter's non-uniform color.

Preliminary camera calibration by distant marble movie images should be sufficient to determine systematic centroid alignment effects.

## 4.2 Close-Up Images Require Modeling of Spacecraft Motion

Centroids can align in an excellent way, but limbs align poorly. The calibration method adjusts the model parameter FramesPerRot, in order to adjust for spacecraft motion and possible color asymmetry, with the obsrved effect at the limbs. See figure 5.

- FramesPerRot=81.055960
- ScaleFactor=1478.000000
- CenterX=815.646902
- CenterY=621.047285
- K1=-0.000000038000000
- K2=0.000000000000002600000000
- RotOffsetZ=0.003562
- ScaleErrorRed=0.000000000000
- ScaleErrorBlue=0.000000000000
- ScaleErrorY=0.000000000000
- x0=769.269856
- y0=750.189299
- x1=769.270970
- y1=750.190248

- x2=769.271840
- y2=750.187521

Figure 5: Post-calibration rendition of perijove-08 approach image JNCE_2017244_08C00057_V01-raw. It shows some misalignment at the limbs, despite excellent centroid alignment. Credit: NASA / JPL-Caltech / SwRI / MSSS / Gerald Eichstädt.

## 4.3 Dependency from Rendering Parameters

The position of the centroids as a function of background subtraction and gamma stretch remains to be investigated. Do camera artifacts play a significant role? Comparing unpatched with patched results can resolve this question. Effects of the particular decompanding method, of lossy data compression, point noise filtering, TDI, stray light remain to be investigated, or ruled out as relevant.

## 4.4 From an Underdetermined to an Overdetermined Method

RGB alignment of the centroid of a single marble movie image is highly accurate, since the method is underdetermined, i.e. the family of camera models has more degrees of freedom than the calibration method is able to nail down. There are several conceivable approaches to overcome this weekness. One of them is minimizing the sum of squares of misalignments

$$\frac{1}{m} \cdot \sum_{i=1}^{m} \Big( (r_{m,x} - g_{m,x})^2 + (r_{m,y} - g_{m,y})^2 + (b_{m,x} - g_{m,x})^2 + (b_{m,y} - g_{m,y})^2 \Big) \tag{7}$$

over $m$ marble movie images. As long as less than four degrees of freedom are added with each marble movie image, this method has at least the theoretical potential to nail down several more geometrical camera parameters.

There are several options to combine a fixed number of centroid-based calibrations. One of them is using PJ08 images that show Io and Europa. Aligning centroids of both moons at once reduced the degrees of freedom by eight.

The blue marble movie image JNCE_2016194_00B1823_V01 shows Jupiter twice. This can be used to determine Juno's rotation period in terms of interframe delay. Assuming a constant interframe delay over consecutive marble movie images, this value can be assumed as a known, when calibrating e.g. with color images #1822 or #1824.

When using other sources, like SPICE, the absolute centroid position of Jupiter can be estimated by rendering a theoretical reference Jupiter image. This narrows down an additional two degrees of freedom for each marble movie image.

Instead of an RMS method, the parameter manifolds with zero centroid alignment error can be approximated for more than one marble movie image. Intersecting these manifolds explictely reduces the dimension of the manifolds, provided the number of degrees of freedom added by each marble movie image is smaller than the number of degrees of freedom the RGB alignment of one marble movie nails down. The manifold may turn out to be sufficiently smooth to be approximated by hyperplanes. This opens an approach with linear methods based on the full Jacobi matrix considering all modeled camera parameters.

# 5 Determining Juno's Rotation Period

## 5.1 Spy Files

The following eight spy-scripts are run with the `spy.exe` tool of the NAIF/SPICE tool set:

```
SAVE TO ..\spyout\spy_results_pj08_v01_Jupiter_SUN_JUPITER.txt;

LOAD \juno\spice\kernels\lsk\naif0012_dos.tls;
LOAD \juno\spice\kernels\sclk\JNO_SCLKSCET.00064_dos.tsc;
LOAD \juno\spice\kernels\fk\juno_v12_dos.tf;
LOAD \juno\spice\kernels\pck\pck00010_dos.tpc;
LOAD \juno\spice\kernels\ck\juno_sc_rec_170820_170826_v01.bc;
LOAD \juno\spice\kernels\ck\juno_sc_rec_170827_170902_v01.bc;
LOAD \juno\spice\kernels\ck\juno_sc_rec_170903_170909_v01.bc;
LOAD \juno\spice\kernels\spk\spk_rec_170728_170918_170922.bsp;


SET START TIME 2017-08-26T09:00:00.000;
SET STOP TIME 2017-09-06T23:00:00.000;
SET STEP SIZE 300.0;
SET TIME FORMAT YYYY-MM-DDTHR:MN:SC.###;
SET OBSERVER JUPITER;
SET TARGET SUN;
SET FRAME IAU_JUPITER;
SET PAGE WIDTH 255;
SET NUMBER FORMAT F20.8;
SHOW ALL;

SAMPLE POSITION;

SAVE TO ..\spyout\spy_results_pj08_v01_Jupiter_SUN_J2000.txt;

LOAD \juno\spice\kernels\lsk\naif0012_dos.tls;
LOAD \juno\spice\kernels\sclk\JNO_SCLKSCET.00064_dos.tsc;
LOAD \juno\spice\kernels\fk\juno_v12_dos.tf;
LOAD \juno\spice\kernels\pck\pck00010_dos.tpc;
LOAD \juno\spice\kernels\ck\juno_sc_rec_170820_170826_v01.bc;
LOAD \juno\spice\kernels\ck\juno_sc_rec_170827_170902_v01.bc;
LOAD \juno\spice\kernels\ck\juno_sc_rec_170903_170909_v01.bc;
LOAD \juno\spice\kernels\spk\spk_rec_170728_170918_170922.bsp;
```

```
SET START TIME 2017-08-26T09:00:00.000;
SET STOP TIME 2017-09-06T23:00:00.000;
SET STEP SIZE 300.0;
SET TIME FORMAT YYYY-MM-DDTHR:MN:SC.###;
SET OBSERVER JUPITER;
SET TARGET SUN;
SET FRAME J2000;
SET PAGE WIDTH 255;
SET NUMBER FORMAT F20.8;
SHOW ALL;

SAMPLE POSITION;

SAVE TO ..\spyout\spy_results_pj08_v01_JUPITER_JUNO_JUNOCAM.txt;

LOAD \juno\spice\kernels\lsk\naif0012_dos.tls;
LOAD \juno\spice\kernels\sclk\JNO_SCLKSCET.00064_dos.tsc;
LOAD \juno\spice\kernels\fk\juno_v12_dos.tf;
LOAD \juno\spice\kernels\pck\pck00010_dos.tpc;
LOAD \juno\spice\kernels\ck\juno_sc_rec_170820_170826_v01.bc;
LOAD \juno\spice\kernels\ck\juno_sc_rec_170827_170902_v01.bc;
LOAD \juno\spice\kernels\ck\juno_sc_rec_170903_170909_v01.bc;
LOAD \juno\spice\kernels\spk\spk_rec_170728_170918_170922.bsp;


SET START TIME 2017-08-26T09:00:00.000;
SET STOP TIME 2017-09-06T23:00:00.000;
SET STEP SIZE 300.0;
SET TIME FORMAT YYYY-MM-DDTHR:MN:SC.###;
SET OBSERVER JUNO;
SET TARGET JUPITER;
SET FRAME JUNO_JUNOCAM;
SET PAGE WIDTH 255;
SET NUMBER FORMAT F20.8;
SHOW ALL;

SAMPLE POSITION;

SAVE TO ..\spyout\spy_results_pj08_v01_JUPITER_J2000.txt;

LOAD \juno\spice\kernels\lsk\naif0012_dos.tls;
LOAD \juno\spice\kernels\sclk\JNO_SCLKSCET.00064_dos.tsc;
LOAD \juno\spice\kernels\fk\juno_v12_dos.tf;
LOAD \juno\spice\kernels\pck\pck00010_dos.tpc;
```

```
LOAD \juno\spice\kernels\ck\juno_sc_rec_170820_170826_v01.bc;
LOAD \juno\spice\kernels\ck\juno_sc_rec_170827_170902_v01.bc;
LOAD \juno\spice\kernels\ck\juno_sc_rec_170903_170909_v01.bc;
LOAD \juno\spice\kernels\spk\spk_rec_170728_170918_170922.bsp;


SET START TIME 2017-08-26T09:00:00.000;
SET STOP TIME 2017-09-06T23:00:00.000;
SET STEP SIZE 300.0;
SET TIME FORMAT YYYY-MM-DDTHR:MN:SC.###;
SET OBSERVER JUNO;
SET TARGET JUPITER;
SET FRAME J2000;
SET PAGE WIDTH 255;
SET NUMBER FORMAT F20.8;
SHOW ALL;

SAMPLE POSITION;

SAVE TO ..\spyout\spy_results_pj08_v01_Jupiter_EARTH_JUPITER.txt;

LOAD \juno\spice\kernels\lsk\naif0012_dos.tls;
LOAD \juno\spice\kernels\sclk\JNO_SCLKSCET.00064_dos.tsc;
LOAD \juno\spice\kernels\fk\juno_v12_dos.tf;
LOAD \juno\spice\kernels\pck\pck00010_dos.tpc;
LOAD \juno\spice\kernels\ck\juno_sc_rec_170820_170826_v01.bc;
LOAD \juno\spice\kernels\ck\juno_sc_rec_170827_170902_v01.bc;
LOAD \juno\spice\kernels\ck\juno_sc_rec_170903_170909_v01.bc;
LOAD \juno\spice\kernels\spk\spk_rec_170728_170918_170922.bsp;


SET START TIME 2017-08-26T09:00:00.000;
SET STOP TIME 2017-09-06T23:00:00.000;
SET STEP SIZE 300.0;
SET TIME FORMAT YYYY-MM-DDTHR:MN:SC.###;
SET OBSERVER JUPITER;
SET TARGET EARTH;
SET FRAME IAU_JUPITER;
SET PAGE WIDTH 255;
SET NUMBER FORMAT F20.8;
SHOW ALL;

SAMPLE POSITION;
```

```
SAVE TO ..\spyout\spy_results_pj08_v01_Jupiter_EARTH_J2000.txt;

LOAD \juno\spice\kernels\lsk\naif0012_dos.tls;
LOAD \juno\spice\kernels\sclk\JNO_SCLKSCET.00064_dos.tsc;
LOAD \juno\spice\kernels\fk\juno_v12_dos.tf;
LOAD \juno\spice\kernels\pck\pck00010_dos.tpc;
LOAD \juno\spice\kernels\ck\juno_sc_rec_170820_170826_v01.bc;
LOAD \juno\spice\kernels\ck\juno_sc_rec_170827_170902_v01.bc;
LOAD \juno\spice\kernels\ck\juno_sc_rec_170903_170909_v01.bc;
LOAD \juno\spice\kernels\spk\spk_rec_170728_170918_170922.bsp;


SET START TIME 2017-08-26T09:00:00.000;
SET STOP TIME 2017-09-06T23:00:00.000;
SET STEP SIZE 300.0;
SET TIME FORMAT YYYY-MM-DDTHR:MN:SC.###;
SET OBSERVER JUPITER;
SET TARGET EARTH;
SET FRAME J2000;
SET PAGE WIDTH 255;
SET NUMBER FORMAT F20.8;
SHOW ALL;

SAMPLE POSITION;


SAVE TO ..\spyout\spy_results_pj08_v01_EARTH_JUNO_JUNOCAM.txt;

LOAD \juno\spice\kernels\lsk\naif0012_dos.tls;
LOAD \juno\spice\kernels\sclk\JNO_SCLKSCET.00064_dos.tsc;
LOAD \juno\spice\kernels\fk\juno_v12_dos.tf;
LOAD \juno\spice\kernels\pck\pck00010_dos.tpc;
LOAD \juno\spice\kernels\ck\juno_sc_rec_170820_170826_v01.bc;
LOAD \juno\spice\kernels\ck\juno_sc_rec_170827_170902_v01.bc;
LOAD \juno\spice\kernels\ck\juno_sc_rec_170903_170909_v01.bc;
LOAD \juno\spice\kernels\spk\spk_rec_170728_170918_170922.bsp;


SET START TIME 2017-08-26T09:00:00.000;
SET STOP TIME 2017-09-06T23:00:00.000;
SET STEP SIZE 300.0;
SET TIME FORMAT YYYY-MM-DDTHR:MN:SC.###;
SET OBSERVER JUNO;
SET TARGET EARTH;
```

```
SET FRAME JUNO_JUNOCAM;
SET PAGE WIDTH 255;
SET NUMBER FORMAT F20.8;
SHOW ALL;

SAMPLE POSITION;

SAVE TO ..\spyout\spy_results_pj08_v01_EARTH_J2000.txt;

LOAD \juno\spice\kernels\lsk\naif0012_dos.tls;
LOAD \juno\spice\kernels\sclk\JNO_SCLKSCET.00064_dos.tsc;
LOAD \juno\spice\kernels\fk\juno_v12_dos.tf;
LOAD \juno\spice\kernels\pck\pck00010_dos.tpc;
LOAD \juno\spice\kernels\ck\juno_sc_rec_170820_170826_v01.bc;
LOAD \juno\spice\kernels\ck\juno_sc_rec_170827_170902_v01.bc;
LOAD \juno\spice\kernels\ck\juno_sc_rec_170903_170909_v01.bc;
LOAD \juno\spice\kernels\spk\spk_rec_170728_170918_170922.bsp;


SET START TIME 2017-08-26T09:00:00.000;
SET STOP TIME 2017-09-06T23:00:00.000;
SET STEP SIZE 300.0;
SET TIME FORMAT YYYY-MM-DDTHR:MN:SC.###;
SET OBSERVER JUNO;
SET TARGET EARTH;
SET FRAME J2000;
SET PAGE WIDTH 255;
SET NUMBER FORMAT F20.8;
SHOW ALL;

SAMPLE POSITION;
```

## 5.2 Selecting Vectors

The output file `spy_results_pj08_v01_EARTH_J2000.txt` contains a line

```
2017-08-27T10:05:00.000
 850637184.89526725 309403045.11710411 115064679.97264077
```

It corresponds to a trajectory point at ISO time `2017-08-27T10:05:00.000`. A similar line is extracted from each of the eight spy-outputs for the same ISO time, resulting in the eight vectors

```
73480.60573969 3904387.85185212 1812863.59408533
```

```
850637184.89526725 309403045.11710411 115064679.97264077
-1580567.19259611 1395084.17289434 -3753886.76015923
-912396671.53284132 3930741.23273347 -8402873.35625181

850563704.28952765 305498657.26525199 113251816.37855543
714612809.19946539 366084242.61353719 139517021.16372886
305303192.47555655 857128188.50366771 -41656304.38830633
166817215.15543187 796592170.12292540 -42036533.90699159
```

These vectors are used to infer all necessary transformations between coordinate systems.

## 5.3 Rendering Masked Jupiter Images

From the above vectors, Jupiter's one bar MacLaurin spheroid, and an assumed camera model, together with some manual corrections, a mask can be rendered, where a rendered Jupiter image should fit in exactly. Juno's rotation period is considered as a parameter of the camera model. A reference time a few minutes away from the nearest actual image avoids ambiguities of the thus far only semi-automatically determined rotation period.

Figure 6 shows a semi-panorama of a masked Jupiter marble rendition. Figure 7 shows crop thereof, 8-fold enlarged. The resolution of the rendition has been 10 pixels per degree. Note, that the camera has a resolution of about 30 pixels per degree.

Images from #07C00543 of ISO time 2017-08-26T09:00:33.114 to #07C00601 of ISO time 2017-08-26T23:30:17.396 showed a good consistence with an assumed constant Juno rotation period of 30.164400 seconds, using SPICE trajectory vectors of 2017-08-26T10:05:00.000 as a reference system.

The time span of 13.5 hours relative to the reference system results in 13.5 hours $\times$ approximately 120 Juno rotations, hence about 1620 rotations, or $1620 \cdot 3600$ pixels = 5832000 pixels, for rendition with 10 pixels per degree. A relative error of the rotaton period of $10^{-6}$ hence shows up in a vertical displacement of the mask relative to the rendered image of 5 to 6 pixels. Visually, errors of about half a pixel can be discerned pretty readily. However, Juno's rotations appears to fluctuate a bit, such that a highly accurate determination of Juno's rotation period down to an accuracy of less then 10 microseconds doesn't seem to make much sense in the context of this article.

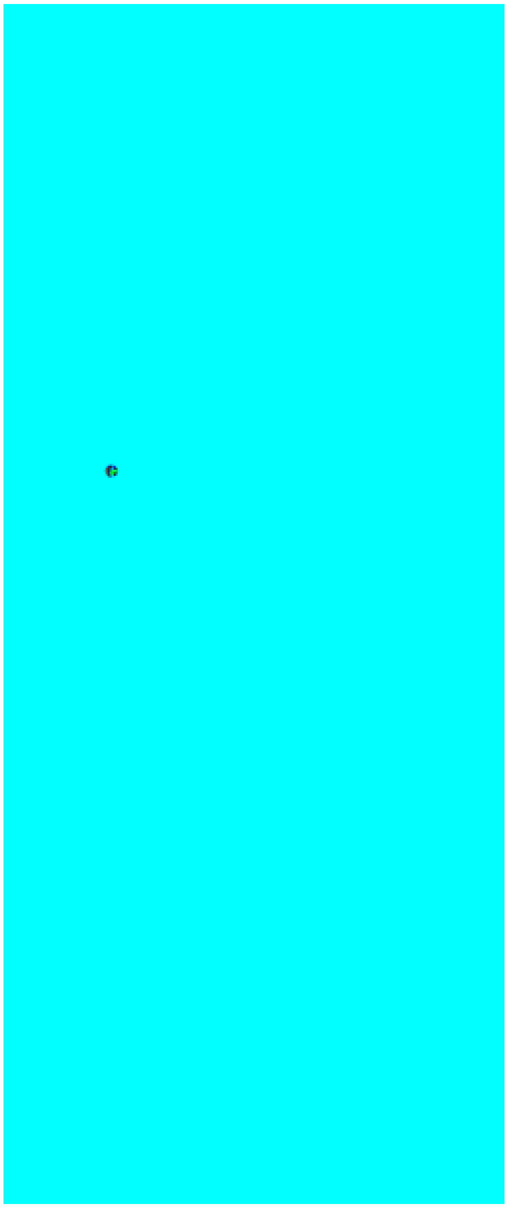

Figure 6: Masked rendered image #07C00603, vertical fov 180 degrees, horizontal fov 75 degrees. Credit: NASA / JPL-Caltech / SwRI / MSSS / Gerald Eichstädt.

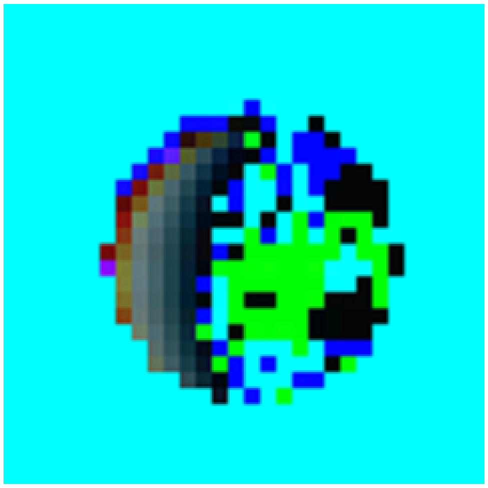

Figure 7: Masked rendered image #07C00603, 10 pixels per degree, crop, 8-fold enlarged. Credit: NASA / JPL-Caltech / SwRI / MSSS / Gerald Eichstädt.

# 6 Selected Preliminary Results

## 6.1 Experiments with Chromatic Aberration for Blue Channel

This short series of experiments with early inbound PJ08 marble movie images assumes

- FramesPerRot=80.870000. This value is derived from a rather accurate determination of a Juno rotation period of 30.164400 seconds, and 0.373 seconds interframe delay as provided by the metadata `JNCE_2017238_07C00543_V01.json`, corrected by one millisecond according to the SPICE instrument kernel `juno_junocam_v02.ti`. A presumed tiny change to 30.164475 seconds per Juno rotation, beginning with #07C00603, doesn't change FramesPerRot significantly.
- ScaleFactor unknown, but should be near 1478.0.
- CenterX unknown, but expected to be near 814.0.
- CenterY unknown, but roughly near 600.0.
- K1=-0.000000038000000.
- K2=0.000000000000002600000000.
- RotOffsetZ unknown, but amount should be smaller than 0.01.
- ScaleErrorRed=0.000000000000.
- ScaleErrorBlue unknown, to be determined approximately.
- ScaleErrorY=0.000000000000.

For image #07C00543, setting ScaleErrorBlue=0.0 resulted in

- ScaleFactor=1477.461529.
- CenterX=833.221607.
- CenterY=611.607528.
- RotOffsetZ=0.002110.

This assumption wasn't explored any further, since CenterX is too far off the expected value.

For image #07C00543, setting ScaleErrorBlue=0.001 resulted in

- ScaleFactor=1472.719008.
- CenterX=772.976249.

- CenterY=613.817608.
- RotOffsetZ=-0.000434.

This assumption wasn't explored any further, neither, since CenterX is again too far off the expected value, but in the opposite direction, this time.

Linear interpolation suggests a value of ScaleErrorBlue=0.0003. Applying the calibration with this assumnption for RGB images #07C00543 to #07C00611 returned:

| image # | ScaleFactor | CenterX | CenterY | RotOffsetZ |
|---|---|---|---|---|
| 07C00543 | 1475.874844 | 813.530567 | 612.239177 | 0.001246 |
| 07C00545 | 1475.986118 | 811.198694 | 610.596265 | 0.000834 |
| 07C00547 | 1476.280887 | 812.251536 | 610.157202 | 0.000763 |
| 07C00549 | 1476.245193 | 810.993811 | 609.438131 | 0.000688 |
| 07C00551 | 1476.693527 | 813.568369 | 609.081074 | 0.000644 |
| 07C00553 | 1476.370881 | 815.526385 | 612.582527 | 0.001437 |
| 07C00555 | 1476.160662 | 811.916767 | 612.138368 | 0.001214 |
| 07C00557 | 1476.565435 | 814.552532 | 611.329713 | 0.001118 |
| 07C00559 | 1476.322136 | 811.892018 | 611.253317 | 0.001069 |
| 07C00561 | 1476.559907 | 813.081075 | 609.469176 | 0.000742 |
| 07C00593 | 1476.818953 | 815.225972 | 611.458369 | 0.001209 |
| 07C00595 | 1476.942818 | 816.933438 | 612.218129 | 0.001398 |
| 07C00597 | 1476.583171 | 814.546662 | 612.436393 | 0.001351 |
| 07C00599 | 1477.129579 | 815.408849 | 610.006063 | 0.000900 |
| 07C00601 | 1477.080499 | 817.336239 | 610.902811 | 0.001105 |
| 07C00603 | 1477.030322 | 815.210574 | 609.107326 | 0.000663 |
| 07C00605 | 1476.772789 | 816.765251 | 612.771134 | 0.001501 |
| 07C00607 | 1477.211708 | 816.921436 | 609.071947 | 0.000752 |
| 07C00609 | 1477.130115 | 816.991473 | 609.610557 | 0.000858 |
| 07C00611 | 1476.404042 | 814.013277 | 612.537499 | 0.001390 |

Figure 8 represents these values as diagrams. This reveals an apparent correlation of ScaleFactor with OpticalAxisX, and of OpticalAxisY with RotOffsetZ. Figure 9 makes this presumed correlation more explicite.

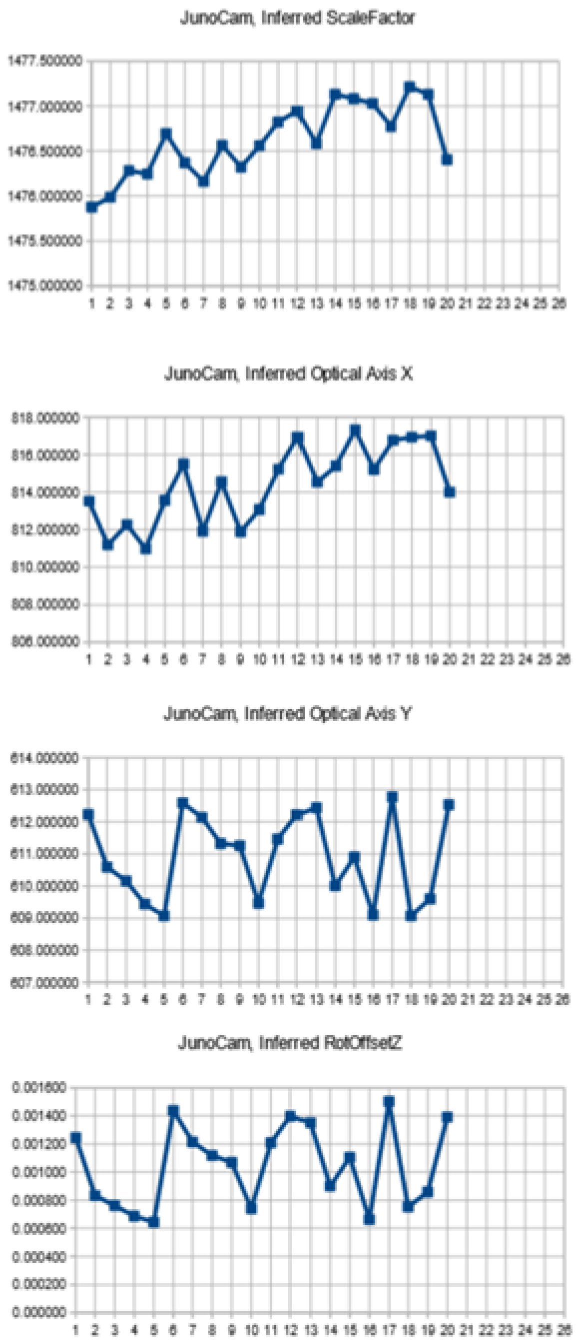


Figure 8: Graphical representation of perijove-08 approach calibration run with an assumed chromatic error of 0.0003 for the blue channel. Credit: NASA / JPL-Caltech / SwRI / MSSS / Gerald Eichstädt.

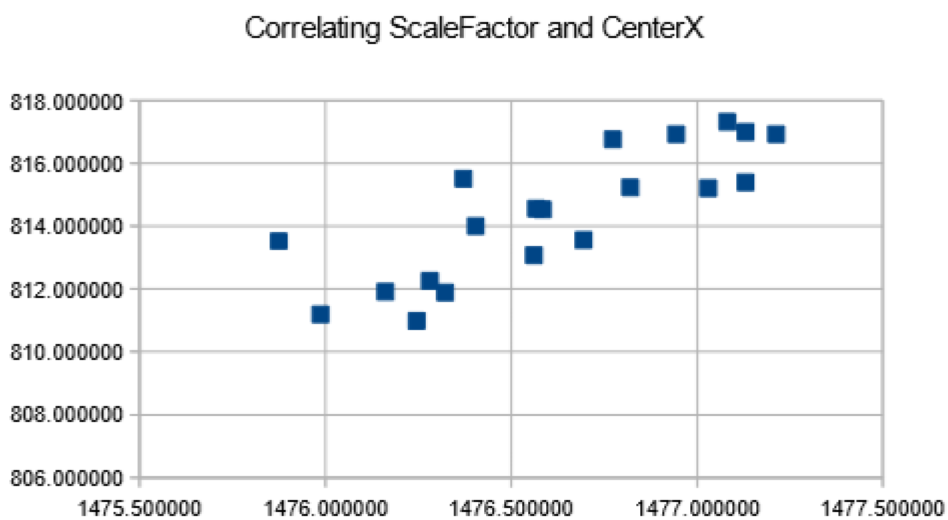


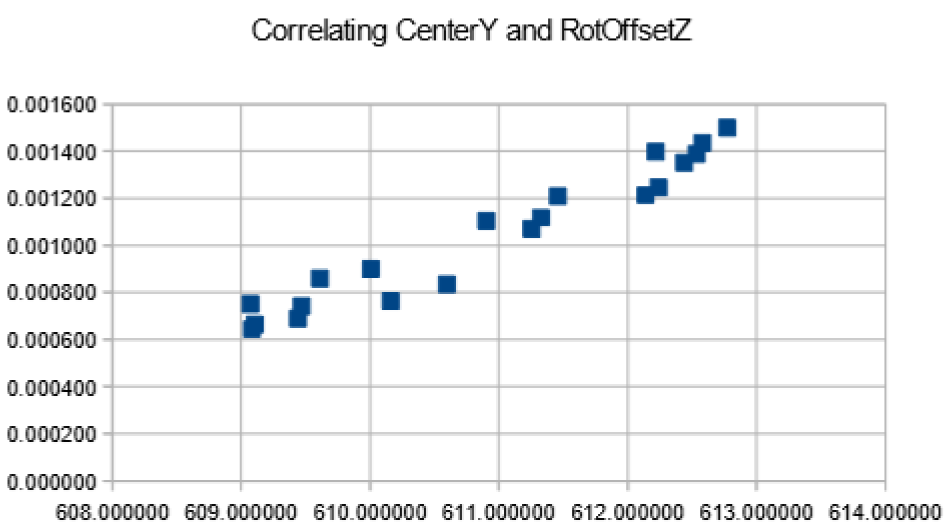


Figure 9: Graphical representation of the correlation between inferred parameters of perijove-08 approach calibration run with an assumed chromatic error of 0.0003 for the blue channel. Credit: NASA / JPL-Caltech / SwRI / MSSS / Gerald Eichstädt.

## 6.2 Experiment with Chromatic Aberration for Red and Blue

This experiment with early inbound PJ08 marble movie images assumes

- FramesPerRot=80.870000.
- ScaleFactor unknown, but should be near 1478.0.
- CenterX=814.0.
- CenterY=600.0.
- K1=-0.000000038000000.
- K2=0.000000000000002600000000.
- RotOffsetZ unknown, but amount should be smaller than 0.01.
- ScaleErrorRed unknown.
- ScaleErrorBlue unknown.
- ScaleErrorY=0.000000000000.

The according calibration run suggests a chromatic aberration for the red channel rather than the blue channel. This might hint towards a correlation between the chosen y-position of the optical axis, and the chromatic aberration of the red and blue channels with respect to the green channel within the context of the assumptions about the other model parameters.

The diagrams of figure 10 don't suggest a strong correlation between the inferred parameters of the according calibration run.

For RGB images #07C00543 to #07C00621 returned the following values in detail:

| image # | ScaleFactor | RotOffsetZ | ScaleErrorRed | ScaleErrorBlue |
|---|---|---|---|---|
| 07C00543 | 1476.398833 | 0.000843 | 0.000742582927 | 0.000029873392 |
| 07C00545 | 1476.575966 | 0.000490 | 0.000693787673 | -0.000153509582 |
| 07C00547 | 1476.572078 | 0.000550 | 0.000697539180 | -0.000003761767 |
| 07C00549 | 1476.823991 | 0.000617 | 0.000588613112 | 0.000013821956 |
| 07C00551 | 1477.167380 | 0.000634 | 0.000486185116 | 0.000012396413 |
| 07C00553 | 1476.826791 | 0.001470 | 0.000702083354 | -0.000722962549 |
| 07C00555 | 1476.777251 | 0.000896 | 0.000755590802 | 0.000018452561 |
| 07C00557 | 1476.808391 | 0.000560 | 0.000773732317 | 0.000145756702 |
| 07C00559 | 1476.787236 | 0.000889 | 0.000762030461 | -0.000288706216 |
| 07C00561 | 1477.054688 | 0.000484 | 0.000534686725 | -0.000252252282 |
| 07C00593 | 1477.180206 | 0.000872 | 0.000724342129 | -0.000006054623 |
| 07C00595 | 1477.393471 | 0.000881 | 0.000636701529 | -0.000397310030 |
| 07C00597 | 1477.120584 | 0.000576 | 0.000714808529 | -0.000180529812 |
| 07C00599 | 1477.525738 | 0.000717 | 0.000542778102 | -0.000017329985 |
| 07C00601 | 1477.081128 | 0.000413 | 0.000720852235 | 0.000055504660 |
| 07C00603 | 1477.195263 | 0.000098 | 0.000582640514 | 0.000006274651 |
| 07C00605 | 1476.904718 | 0.000841 | 0.000882865324 | 0.000015141798 |
| 07C00607 | 1477.250834 | 0.000128 | 0.000588644123 | 0.000019979678 |
| 07C00609 | 1477.315584 | 0.000396 | 0.000568496564 | -0.000173427874 |
| 07C00611 | 1476.733250 | 0.000772 | 0.000819249197 | 0.000016835570 |
| 07C00613 | 1476.862923 | 0.000733 | 0.000756715485 | -0.000241857738 |
| 07C00615 | 1477.056223 | 0.000404 | 0.000541748789 | 0.000011488594 |
| 07C00617 | 1477.149211 | 0.000405 | 0.000710311636 | 0.000027141193 |
| 07C00619 | 1477.208110 | 0.000366 | 0.000673080414 | 0.000022110739 |
| 07C00621 | 1476.708367 | 0.000959 | 0.000938836643 | 0.000012940330 |

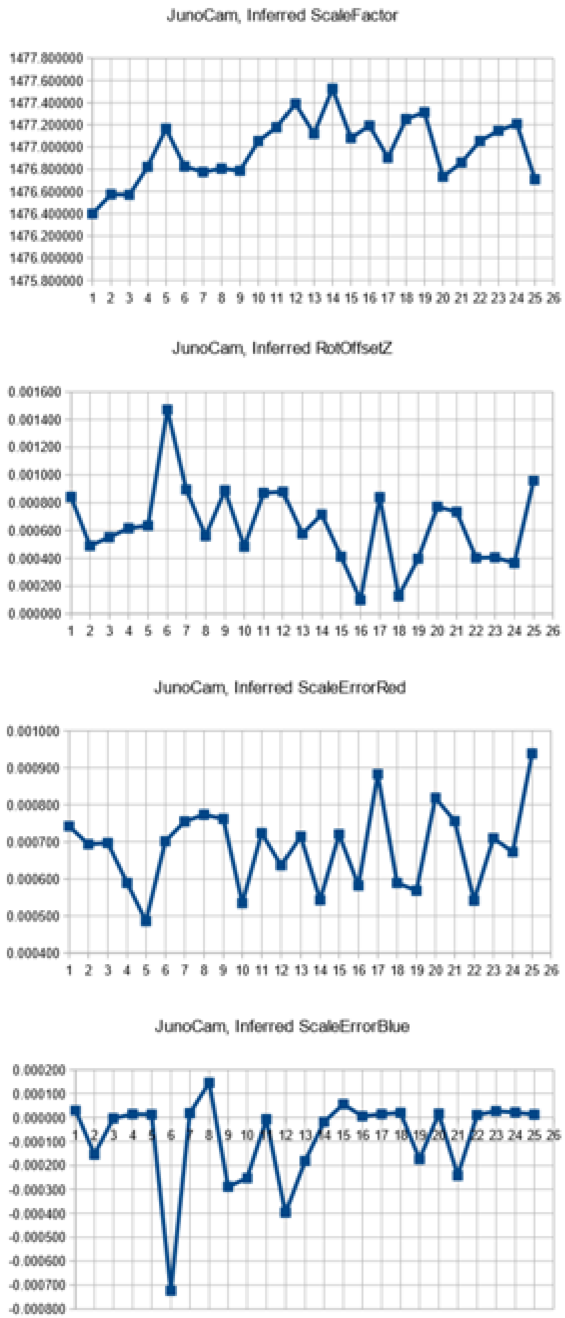


Figure 10: Graphical representation of a perijove-08 approach calibration run with a fixed optical axis at x=814.0, and y=600.0. Credit: NASA / JPL-Caltech / SwRI / MSSS / Gerald Eichstädt.

## 6.3 Using Best-Fit Calibrations Obtained from Star Images

Two calibration runs have been performed with parameters derived from a JunoCam instrument kernel provided by SPICE. This kernel is based on a best-fit model for cruise images of stars.

### 6.3.1 ScaleFactor Inferred

A first calibration run is based on the following assumptions:

- FramesPerRot=80.870000.
- ScaleFactor unknown, but should be near 1478.0.
- CenterX=814.210000.
- CenterY=596.520000.
- K1=-0.000000059624209.
- K2=0.000000000000027381910.
- RotOffsetZ unknown, but amount should be smaller than 0.01.
- ScaleErrorRed unknown.
- ScaleErrorBlue unknown.
- ScaleErrorY=0.000000000000.

Note, that the Browinan distortion parameter K1 is almost doubled, and the paramter K2 more than the 10-fold of the previous runs.

The calibration run failed for the second iteration step. So here the results after the first iteration of the pseudo-Newton method, with a non-negligible residual misalignment:

| image # | ScaleFactor | RotOffsetZ | ScaleErrorRed | ScaleErrorBlue |
|---|---|---|---|---|
| 07C00543 | 1472.692398 | 0.001650 | -0.002088394864 | -0.001009777013 |
| 07C00545 | 1473.158619 | 0.000666 | -0.002723750743 | -0.000628234869 |
| 07C00547 | 1473.615179 | 0.001328 | -0.002404507511 | -0.000601612511 |
| 07C00549 | 1473.288607 | 0.000995 | -0.002318764700 | -0.000797203112 |
| 07C00551 | 1473.159639 | -0.000016 | -0.002137751013 | -0.000494675984 |
| 07C00553 | 1472.891475 | 0.000257 | -0.002067897007 | -0.000617778975 |
| 07C00555 | 1473.063519 | 0.001780 | -0.002062010497 | -0.001018603276 |
| 07C00557 | 1473.167377 | 0.000225 | -0.002939236957 | -0.000429156086 |
| 07C00559 | 1473.180332 | 0.001344 | -0.002280193146 | -0.000865660381 |
| 07C00561 | 1473.759742 | -0.000346 | -0.002620647081 | -0.000461307413 |
| 07C00593 | 1473.030104 | 0.001782 | -0.001958780192 | -0.001021079473 |
| 07C00595 | 1473.395192 | 0.000624 | -0.002114741583 | -0.000714900251 |
| 07C00597 | 1472.799739 | 0.001276 | -0.002445466978 | -0.000781882607 |
| 07C00599 | 1473.177612 | 0.000250 | -0.002078307224 | -0.000561419115 |
| 07C00601 | 1473.898884 | 0.002459 | -0.002135865459 | -0.000930617115 |
| 07C00603 | 1473.516094 | 0.000844 | -0.002809626646 | -0.000596992159 |
| 07C00605 | 1473.730362 | 0.000689 | -0.002768668952 | -0.000612843554 |
| 07C00607 | 1473.709410 | 0.000922 | -0.002820883809 | -0.000635008199 |
| 07C00609 | 1472.581345 | 0.001843 | -0.001966392310 | -0.001063515669 |
| 07C00611 | 1473.121701 | 0.002818 | -0.001940113552 | -0.000995213369 |
| 07C00613 | 1473.021214 | 0.000848 | -0.002471801758 | -0.000689619443 |
| 07C00615 | 1472.622573 | 0.002251 | -0.001744779956 | -0.001229461774 |
| 07C00617 | 1473.851932 | 0.001833 | -0.002452013637 | -0.000846404720 |
| 07C00619 | 1473.608160 | 0.001519 | -0.002393176908 | -0.000809886880 |
| 07C00621 | 1473.088310 | 0.000808 | -0.002662043918 | -0.000575411277 |

The values are visualized in figure 11.

Here the list of centroid positions in the respective crops, as an idea of the residual misalignments:

| image # | x_red | y_red | x_green | y_green | x_blue | y_blue |
|---|---|---|---|---|---|---|
| 07C00543 | 723.845081 | 669.277097 | 723.988013 | 669.190769 | 723.917751 | 669.366980 |
| 07C00545 | 724.497669 | 659.493782 | 724.452656 | 659.538053 | 724.476167 | 659.527618 |
| 07C00547 | 744.361093 | 723.624832 | 744.357740 | 723.692435 | 744.341100 | 723.692416 |
| 07C00549 | 743.700914 | 715.096725 | 743.838997 | 715.001309 | 743.836503 | 715.027424 |
| 07C00551 | 743.878418 | 708.791138 | 743.863345 | 708.970392 | 743.920889 | 708.944133 |
| 07C00553 | 742.645070 | 716.757828 | 742.759697 | 717.073494 | 742.753976 | 716.968156 |
| 07C00555 | 741.731344 | 722.242393 | 741.759744 | 722.054144 | 741.726536 | 722.224116 |
| 07C00557 | 741.959494 | 723.097266 | 741.584660 | 723.569327 | 741.618819 | 723.674401 |
| 07C00559 | 740.976708 | 712.050510 | 740.971602 | 711.974498 | 740.919150 | 712.094422 |
| 07C00561 | 742.391262 | 704.154714 | 742.455685 | 704.226027 | 742.195328 | 703.871853 |
| 07C00593 | 733.828555 | 696.743186 | 733.844233 | 696.603144 | 733.807965 | 696.898876 |
| 07C00595 | 734.691480 | 688.701562 | 734.747172 | 688.762716 | 734.667057 | 688.658925 |
| 07C00597 | 732.601698 | 690.834023 | 732.683564 | 691.065068 | 732.655464 | 691.340893 |
| 07C00599 | 733.790359 | 684.607503 | 733.737580 | 684.792467 | 733.820984 | 684.825208 |
| 07C00601 | 733.194521 | 696.562610 | 733.361192 | 696.203973 | 733.259592 | 696.239552 |
| 07C00603 | 732.575035 | 685.660358 | 732.640042 | 685.806932 | 732.599837 | 685.912706 |
| 07C00605 | 732.764097 | 684.478050 | 732.692749 | 684.586577 | 732.553841 | 684.388990 |
| 07C00607 | 731.983580 | 691.464058 | 732.183096 | 691.473044 | 732.051265 | 691.533604 |
| 07C00609 | 729.665466 | 699.596031 | 729.840079 | 699.619420 | 729.751441 | 700.231030 |
| 07C00611 | 730.002077 | 695.502733 | 729.984551 | 695.257592 | 729.927388 | 695.452637 |
| 07C00613 | 730.124114 | 681.395772 | 730.076204 | 681.440602 | 730.059278 | 681.473792 |
| 07C00615 | 728.610103 | 687.266805 | 728.629842 | 686.920192 | 728.666985 | 687.483385 |
| 07C00617 | 729.983171 | 692.585842 | 730.236384 | 692.292920 | 730.153254 | 692.253162 |
| 07C00619 | 729.266017 | 685.173525 | 729.422350 | 684.840929 | 729.399948 | 684.819530 |
| 07C00621 | 728.544588 | 678.321056 | 728.202124 | 678.815393 | 728.103871 | 678.855739 |

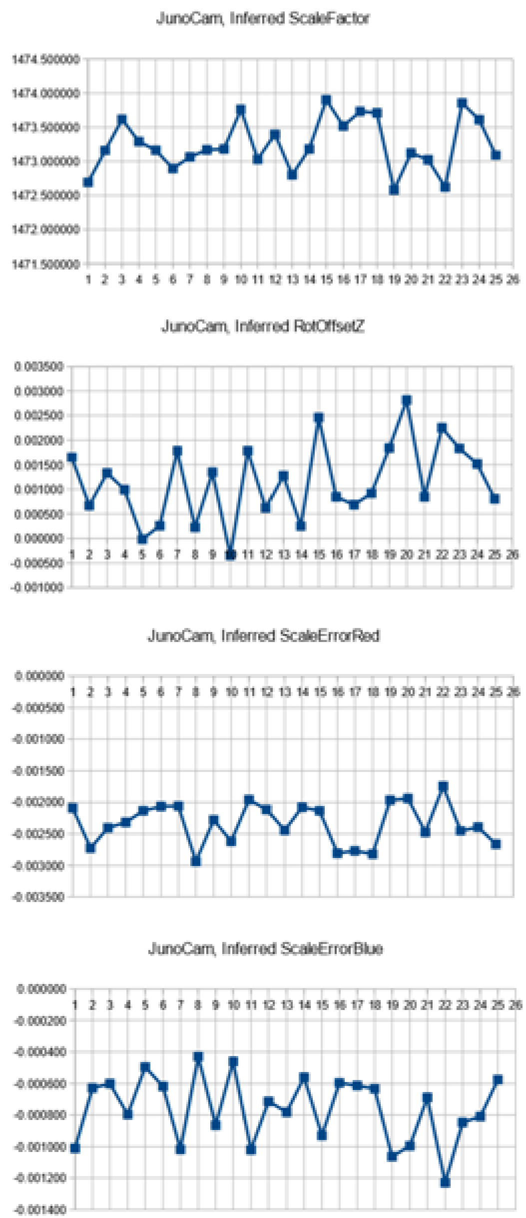


Figure 11: Graphical representation of a perijove-08 approach calibration run with a fixed optical axis at x=814.21, y=596.52, K1=-0.000000059624209, and K2=0.00000000000002738191. Chromatic aberration as well as the ScaleFactor are inferred. Credit: NASA / JPL-Caltech / SwRI / MSSS / Gerald Eichstädt.

### 6.3.2 Non-Square Pixels Allowed

The second calibration run uses the scale factor derived from the instrument kernel, and allows for non-square pixels:

- FramesPerRot=80.870000.
- ScaleFactor=1480.590000.
- CenterX=814.210000.
- CenterY=596.520000.
- K1=-0.000000059624209.
- K2=0.000000000000027381910.
- RotOffsetZ unknown, but amount should be smaller than 0.01.
- ScaleErrorRed unknown.
- ScaleErrorBlue unknown.
- ScaleErrorY=unknown.

The according calibration run returned the following values for the unknown parameters:

| image # | RotOffsetZ | ScaleErrorRed | ScaleErrorBlue | ScaleErrorY |
|---|---|---|---|---|
| 07C00543 | 0.001038 | -0.002278034732 | -0.000794217964 | -0.005257020961 |
| 07C00545 | 0.000607 | -0.002739579549 | -0.000618883824 | -0.005040275808 |
| 07C00547 | 0.001664 | -0.002271488871 | -0.000669858715 | -0.004746010043 |
| 07C00549 | 0.001051 | -0.002260352065 | -0.000799309991 | -0.005087290581 |
| 07C00551 | 0.000282 | -0.002056058095 | -0.000636824173 | -0.004920421280 |
| 07C00553 | 0.000911 | -0.001803802406 | -0.000896965784 | -0.005099553715 |
| 07C00555 | 0.001527 | -0.002126082443 | -0.000927346567 | -0.005021662238 |
| 07C00557 | 0.000121 | -0.002985050228 | -0.000403634492 | -0.004990136998 |
| 07C00559 | 0.000858 | -0.002454402431 | -0.000714155983 | -0.004951576781 |
| 07C00561 | 0.000736 | -0.002210980341 | -0.000688835578 | -0.005101000129 |
| 07C00593 | 0.000698 | -0.002324256170 | -0.000665871000 | -0.004948809459 |
| 07C00595 | 0.001171 | -0.001915395213 | -0.000892128865 | -0.004979852315 |
| 07C00597 | 0.001207 | -0.002447011613 | -0.000759036089 | -0.004892212532 |
| 07C00599 | 0.000029 | -0.002157608671 | -0.000536207467 | -0.004813875110 |
| 07C00601 | 0.000755 | -0.002744165485 | -0.000509431649 | -0.004700561669 |
| 07C00603 | 0.001332 | -0.002554371257 | -0.000686973775 | -0.004702869659 |
| 07C00605 | 0.001961 | -0.002260589179 | -0.000876999386 | -0.004765404311 |
| 07C00607 | 0.000754 | -0.002858511279 | -0.000560159308 | -0.004639364035 |
| 07C00609 | 0.000944 | -0.002168198860 | -0.000772701751 | -0.004982796845 |
| 07C00611 | 0.001632 | -0.002424454372 | -0.000726055486 | -0.004887199522 |
| 07C00613 | 0.000996 | -0.002417282923 | -0.000722429694 | -0.005099670454 |
| 07C00615 | 0.000687 | -0.002282938911 | -0.000742474276 | -0.005150526749 |
| 07C00617 | 0.001391 | -0.002561766732 | -0.000724559395 | -0.004753756919 |
| 07C00619 | 0.001205 | -0.002506356893 | -0.000745041464 | -0.004814703308 |
| 07C00621 | 0.000650 | -0.002710142717 | -0.000507084195 | -0.005129718079 |

The values are visualized in figure 12.

Residual misalignments:

| image # | x_red | y_red | x_green | y_green | x_blue | y_blue |
|---|---|---|---|---|---|---|
| 07C00543 | 736.991776 | 667.445851 | 737.062583 | 667.490639 | 737.054208 | 667.507763 |
| 07C00545 | 736.665643 | 659.289174 | 736.596256 | 659.360308 | 736.607874 | 659.364887 |
| 07C00547 | 755.672833 | 724.659159 | 755.676265 | 724.630818 | 755.673496 | 724.674463 |
| 07C00549 | 755.707958 | 715.142644 | 755.749969 | 715.105666 | 755.783799 | 715.241718 |
| 07C00551 | 755.876864 | 709.813517 | 755.864415 | 709.839560 | 755.864871 | 709.803249 |
| 07C00553 | 755.133835 | 718.972781 | 755.038855 | 718.948274 | 754.998219 | 718.904485 |
| 07C00555 | 754.165690 | 721.534364 | 754.128293 | 721.365521 | 754.131268 | 721.439123 |
| 07C00557 | 754.101448 | 722.788117 | 753.730217 | 723.279467 | 753.771699 | 723.364764 |
| 07C00559 | 753.236664 | 710.558368 | 753.205895 | 710.621367 | 753.183932 | 710.629674 |
| 07C00561 | 753.327782 | 707.081841 | 753.258652 | 707.109843 | 753.326633 | 707.275196 |
| 07C00593 | 746.568812 | 693.480719 | 746.558382 | 693.597859 | 746.547738 | 693.599108 |
| 07C00595 | 746.346134 | 690.316207 | 746.314438 | 690.269398 | 746.297788 | 690.346727 |
| 07C00597 | 745.417205 | 691.074822 | 745.463083 | 691.003390 | 745.441992 | 690.964082 |
| 07C00599 | 745.969822 | 684.115964 | 745.966142 | 684.229501 | 745.908120 | 684.095531 |
| 07C00601 | 744.754860 | 690.989712 | 744.627275 | 691.332624 | 744.626233 | 691.337742 |
| 07C00603 | 744.182080 | 687.376923 | 744.141337 | 687.217242 | 744.151873 | 687.294724 |
| 07C00605 | 743.687492 | 688.456342 | 743.687493 | 688.144204 | 743.654028 | 688.151479 |
| 07C00607 | 743.374974 | 690.955686 | 743.484526 | 690.998897 | 743.451238 | 690.996817 |
| 07C00609 | 743.311123 | 697.325570 | 743.240707 | 697.217122 | 743.149200 | 697.392820 |
| 07C00611 | 742.499068 | 691.858566 | 742.442747 | 691.931125 | 742.402791 | 691.943803 |
| 07C00613 | 742.488584 | 681.886179 | 742.446113 | 681.862670 | 742.453417 | 681.911478 |
| 07C00615 | 742.153703 | 682.540520 | 742.214845 | 682.545132 | 742.164856 | 682.725988 |
| 07C00617 | 741.304321 | 691.018483 | 741.357370 | 690.984512 | 741.330497 | 691.032796 |
| 07C00619 | 740.829020 | 684.047433 | 740.940148 | 683.905737 | 740.881229 | 683.937446 |
| 07C00621 | 740.935605 | 677.745659 | 740.534862 | 678.347398 | 740.511094 | 678.418754 |

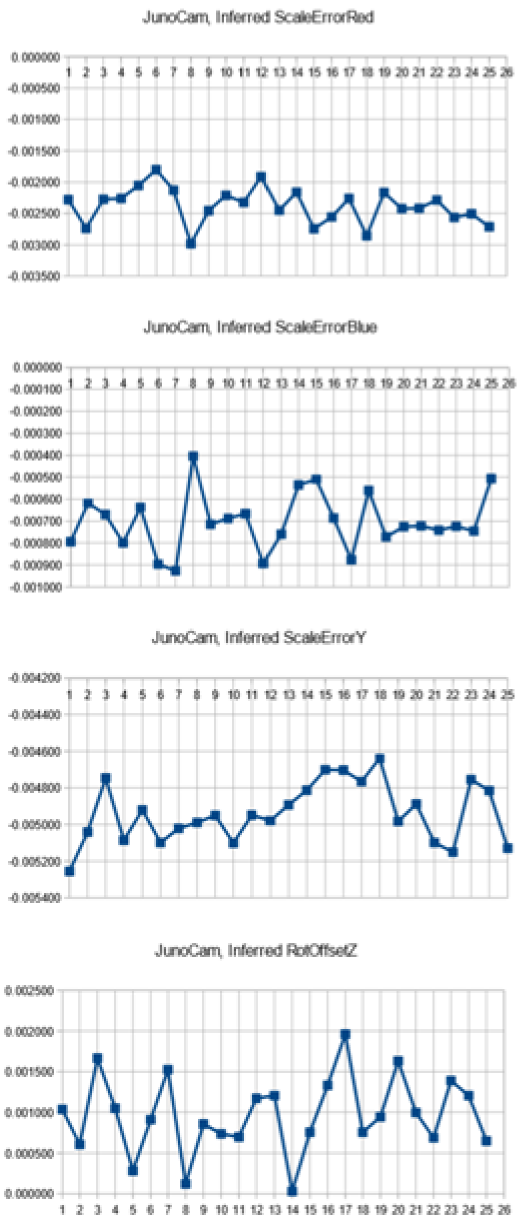


Figure 12: Graphical representation of a perijove-08 approach calibration run with a fixed optical axis at x=814.21, y=596.52, K1=-0.000000059624209, and K2=0.00000000000002738191, ScaleFactor=1480.59. Chromatic aberration as well as the deviation of the pixels from square are inferred. Credit: NASA / JPL-Caltech / SwRI / MSSS / Gerald Eichstädt.

# References

[1] D.C. Brown. *Decentering distortion of lenses.* Photogramm. Eng. 32(3), 444-462 (1966)

[2] A.E. Conrady. *Decentred Lense Sytems.* Monthly Notices of the Royal Astronomical Society, Vol. 79, 1919

[3] C.J. Hansen, M.A. Caplinger, A. Ingersoll, M.A. Ravine, E. Jensen, S. Bolton, G. Orton. *Junocam: Juno's Outreach Camera.* Space Sci Rev DOI 10.1007/s11214-014-0079-x, Springer, 2014

[4] L. Lindegren. *The Astrometric Instrument of Gaia: Principles.* Lund Observatory, Lund University, 22100 Lund, Sweden (2004)

[5] `https://www.missionjuno.swri.edu/junocam/processing`

[6] `naif.jpl.nasa.gov/naif/`

[7] `naif.jpl.nasa.gov/pub/naif/JUNO/kernels/`